DIFFUSER OPTIMIZATION USING COMPUTATIONAL FLUID DYNAMICS AND MICRO-GENETIC ALGORITHMS

Berge Djebedjian

Mechanical Power Engineering Department, Faculty of Engineering,
Mansoura University, El-Mansoura, Egypt
E-Mail: bergedje@mans.edu.eg

تعظيم أداء الناشر باستخدام ديناميكا الموائع العددية والخوارزميات الجينية

الخلاصة:

يقدم هذا البحث طريقة لتعظيم أداء النواشر ذات السريان الاضطرابي. تم تطوير طريقة لتكاما نموذج عددي لديناميكا الموائع الحسابية ذو أساس حجم محدود وأداة تعظيم تستخدم الخوارزميات الجينية . نموذج ديناميكا الموائع العددية مؤسس على معادلات نافير-ستوك مع نموذج الاضطراب k-ε القياسي. هذه الطريقة تم اختبارها على حالتين مختصتين بالانسياب المضطرب. الأولى تحديد طول الناشر المخروطي الذي يعطي أقصى معامل لاستخلاص الضغط الاستاتيكي لنسبة مساحة ناشر وقد أوضحت النتائج أن هناك اتفاقا جيداً مع النتائج المعملية. الحالة الثانية هي تعظيم الأداء من خلال تشكيل السطح لناشر ثنائي الأبعاد معطى له نسبة المساحة ونسبة الطول وقد أوضحت النتائج أنه يمكن تحسين أداء الناشر بهذه الطريقة.

ABSTRACT

An approach for the optimization of turbulent flow in diffusers is presented. A methodology is developed to integrate a finite volume-based computational fluid dynamics (CFD) model and an optimization tool uses micro-genetic algorithms (μ-GA). The CFD model is based on the Reynolds-averaged Navier-Stokes equations, with the standard k-ε closure turbulence model.

This methodology is tested on two cases. The first is the estimation of the conical diffuser length, which gives the maximum pressure recovery coefficient, for a given diffuser area ratio. Good agreement between the computational and experimental results is obtained. The second case is the optimization through wall contouring of a given two-dimensional diffuser area ratio and length ratio. The results indicate that the diffuser performance can be improved by this method.

Keywords: Optimization – Genetic Algorithms – Diffuser – Turbulent Flow

1. INTRODUCTION

Well-designed diffusers should cause minimal total pressure losses and deliver nearly uniform flow at their exits. In some engineering applications, short straight diffusers are demanded for weight and space considerations, resulting in large changes in cross-sectional area. This may develop strong secondary flow and boundary layer separation. Consequently, an increment in the total pressure loss at the diffuser exit is caused.

Experimental studies on the design of symmetric diffusers dealt with the best choice of sizing variables namely: the area ratio AR and the diffuser length to inlet width ratio L/W_1. More sophisticated techniques for reducing or even avoiding flow separation can be found in engineering practice. These techniques include: (i) boundary layer suction, (ii) boundary layer blowing, (iii) insertion of guide vanes, and (iv) wall contouring. The last technique has advantages over the other techniques such as: no auxiliary equipment is required as in methods (i) and (ii) and that the flow passage is not partially blocked as in method (iii).

The use of numerical optimization for laminar and turbulent flow applications has received attention in recent researches. Adventure of high-speed computers and availability of reliable CFD solvers greatly simplify the numerical optimization processes to achieve complex shape designs for optimum performance. It should be mentioned that the accuracy of any optimization process relies on the accuracy of the CFD code, which implies that inaccuracies in the code shade doubt on the outcome of the optimization. For the CFD code, inadequate turbulence modeling might cause the imprecision.

Table 1 shows a summary of previous numerical studies on the optimization of 2-D and conical diffusers for incompressible flow. Three-dimensional S-shaped diffusers (e.g. Lefantzi and Knight [1]) and diffusers with compressible flow are not included.

Çabuk and Modi [2] derived a variational formulation of the problem of determining the profile of a plane diffuser (of given upstream width and length) for a maximum static pressure rise. They obtained the diffuser shape as well as the diffuser width at the exit section. Their results showed that the numerically obtained C_p values for the optimum diffuser were always higher than those for straight diffusers of the same area ratio at several Reynolds numbers in laminar flow regime.

Table 1. Previous numerical studies on diffuser optimization for incompressible flow

Authors, (Year)	Optimization Method	Type of Diffuser	Type of Flow	Reynolds Number	Area Ratio	Ratio L/W₁
Çabuk and Modi (1992), [2]	Adjoint operator method	2-D	Laminar	50 – 500	–	3
Svenningsen et al. (1996), [3]	Sequential linear programming	2-D	Laminar	400	1.68	3.78
Cholaseuk et al. (1999), [4]	Black-box optimization	2-D & Conical	Laminar	50 – 400	–	3
Madsen et al. (1999), [5]	Sequential linear programming	2-D	Turbulent	2×10^5	1.5 – 3	3
Madsen et al. (2000). [6]	Response surface techniques	2-D	Turbulent	2×10^5	2	1.5
Cholaseuk et al. (2000). [7]	Black-box optimization	2-D	Laminar	100	2 – 2.8	3
Eisinger and Ruprecht (2001). [8]	Extrem. Simplex, and genetic methods	Conical	Turbulent	–	4	2 – 12
Lund et al. (2001). [9]	Sequential linear programming	2-D	Turbulent	2×10^5	3	3
Madsen and Langthjem (2001), [10]	Multifidelity response surface approximations	2-D	Turbulent	2×10^5	1.5 – 3.5	1.5

Svenningsen et al. [3] presented an approach to the quasi-analytical sensitivity analysis for CFD problems. The quasi-analytical sensitivity analysis forms a substantial part of an optimization tool based on sequential linear programming. They applied their method on a two-dimensional laminar-flow diffuser to maximize the pressure recovery by altering the wall shape. Compared to a straight-walled diffuser, the optimized shape constituted a minor improvement (3% in C_p).

Cholaseuk et al. [4] and [7] explored the optimum design of fluid flow devices using designed numerical experiments, and the stability (robustness) of such designs, respectively. The search pattern during the optimization process was suggested by the design of experiment methodology. The proposed framework was tested with one potential flow problem and two laminar-flow diffuser problems. Significant improvements in C_p for both plane and conical diffusers were achieved for all studied Reynolds numbers. For example, for a Reynolds number of 100, the initial straight diffuser produced a C_p value of 0.41 while the optimum-profile diffuser produced 0.46.

Madsen et al. [5] presented results from derivative-based design optimization of turbulent flow subsonic diffusers with straight centerline. They considered the two-well known techniques for reducing flow separation, namely: contouring of the diffuser wall and insertion of straight guide vanes. For diffuser designs with small area expansions and no flow separation, the potential gain from optimization was marginal, whereas the pressure recovery of wide-angled diffusers improved substantially.

Madsen et al. [6] used the response surface techniques for design optimization of a two-dimensional diffuser. The wall shape was optimized to achieve maximum pressure recovery, with two different profile representations for the wall. Their analysis resulted in a diffuser design, which was mostly bell shaped with the end of the diffuser wall bent concavely outward. The gain in pressure recovery from optimization was small (1%), as there was a large family of diffusers with essentially identical performance.

Eisinger and Ruprecht [8], in their study of the shape optimization of a turbine draft tube, applied different optimization algorithms, among others, on two axially symmetric diffusers. In the first case, the only optimized parameter was the length of the diffuser while for the second case, a combination of two diffusers, two parameters were optimized: the length and the exit diameter of the first diffuser. The genetic algorithm showed a very robust behavior, but it required a distinctly more optimization cycles and computational time.

Lund et al. [9] studied the wall contouring of a 2-D symmetrical diffuser for maximum pressure recovery. They studied one of the diffusers used by Madsen et al. [5]. The wall contour was described with a B-spline having 5 control points that were allowed to move vertically. The value of C_p was increased from 0.665 to 0.671, i.e., only a small improvement was obtained by changing the wall contour in this case.

Madsen and Langthjem [10] obtained the optimum area ratios AR for fixed-length diffusers using the multifidelity response surface and the sensitivity-based search optimization. In terms of the maximum static pressure recovery, the two optimal designs were practically indistinguishable (C_p-values within 1%).

The objective of the present research is to develop a methodology to integrate a surface representation technique, structured grid generator, a Reynolds-averaged Navier-Stokes solver and a genetic algorithm optimization tool to maximize the static pressure recovery coefficient of subsonic diffusers.

2. OPTIMIZATION LOOP

Optimization methods may be divided into two basic categories, namely, gradient-based, and non-gradient-based. The former category includes the classical steepest descent method, conjugate gradient method and sequential quadratic programming method. These techniques rely upon an accurate estimate of the gradient of the objective function, which may not always be feasible.

Non-gradient-based optimization algorithms require only the evaluation of the objective function for a given design variable. Recent researches have focused on evolutionary algorithms that mimic the Darwinian process of natural evolution to achieve an optimum design. Evolutionary Algorithms have been applied to a broad scope of engineering design problems, and are adopted in the present study.

The automated optimization process is based on the development of several tools linked within a loop algorithm presented in Fig. 1. The heart of the optimization loop, implemented for designing diffusers, is called the optimizer. The automated loop links together an optimizer (optimization algorithm) with a fluid-flow simulator. Declaring the optimization geometrical parameters and implementing the geometry constraints to reduce the computational time, the optimizer generates a candidate diffuser that is described by the geometrical parameters. These values of the parameters are passed to the flow field analysis. This analysis consists of a geometrical processor to describe the studied geometry, a grid generator to create the grid, a flow solver (Reynolds-averaged Navier-Stokes simulations) and a post processor for the presentation of the calculated flow variables. Based on the simulation results, the objective function is calculated. The optimizer generates another candidate diffuser described by new values for the geometrical parameters and the loop continues until an optimum objective function is reached which gives the optimum shape.

The following sections describe the four major points of the automatic optimization procedure, namely: design parameterization, CFD-simulation, objective function, and optimization algorithm.
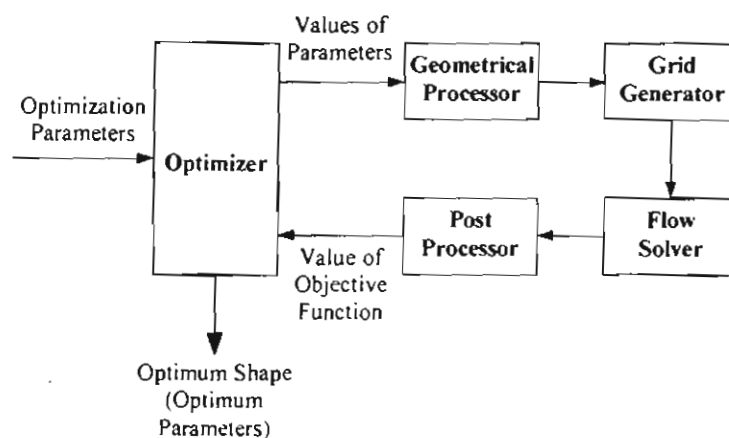

Figure 1. Structure of the mathematical optimization loop

3. DESIGN PARAMETERIZATION

Great importance is given to the parameterization criterion of the diffuser geometry since it affects both the validity and efficiency of the optimization. Describing the diffuser geometry by a large number of parameters is recommended in order to explore a wide range of possibilities in the total search space. However, it is known that the larger the search space, the higher the computational effort.

The details of the diffuser geometry parameterization are given in § 7.2.

4. CFD-SIMULATION

The CAFFA (Computer-Aided Fluid Flow Analysis) (Ferziger and Perić, [11]) Navier-Stokes solver was used in this study to evaluate the performance of the two-dimensional and axisymmetric diffusers. CAFFA is a general purpose CFD code that solves 2D Reynolds-averaged Navier-Stokes equations using a body-fitted finite volume discretization method.

4.1. Governing Equations

The numerical solution of the time-averaged Navier-Stokes equations with the standard k-ε model of turbulence are employed in the present work.

The steady transport equation for a general dependent variable ϕ can be written in two-dimensional and/or axisymmetric form as follows:

$$\frac{\partial}{\partial x}(\rho U \phi) + \frac{1}{r^n}\frac{\partial}{\partial y}\left(r^n \rho V \phi\right) = \frac{\partial}{\partial x}\left(\Gamma_\phi \frac{\partial \phi}{\partial x}\right) + \frac{1}{r^n}\frac{\partial}{\partial y}\left(r^n \Gamma_\phi \frac{\partial \phi}{\partial y}\right) + S_\phi \quad \text{.... (1)}$$

Superscript n of r^n is 1 for axisymmetric and 0 for two-dimensional. Γ_ϕ is the exchange coefficient and S_ϕ is an accumulation of source terms not explicitly represented by the remaining terms of the equation. The dependent variable ϕ can be unity (mass conservation), U or V (momentum conservation), k (turbulence energy), or ε (energy dissipation).

The governing equations for the case of zero tangential velocity, and the constants used in the standard k-ε model (Launder and Spalding, [12]) are given in Tables 2 and 3, respectively.

The isotropic effective viscosity is given by:

$$\mu_{eff} = \mu + \mu_t = \mu + C_\mu \rho \frac{k^2}{\varepsilon} \quad \text{.... (2)}$$

The production of turbulent kinetic energy P is given by:

$$P = \frac{\mu_t}{\rho}\left[\left(\frac{\partial U}{\partial y} + \frac{\partial V}{\partial x}\right)^2 + 2\left(\frac{\partial U}{\partial x}\right)^2 + 2\left(\frac{\partial V}{\partial y}\right)^2 + 2n\left(\frac{V}{r}\right)^2\right] \quad \text{.... (3)}$$

Table 2. Transport equations

Equation	ϕ	Γ_ϕ	S_ϕ
Continuity	1	0	0
x-momentum	U	μ_{eff}	$-\frac{\partial p}{\partial x}+\frac{\partial}{\partial x}\left(\mu_{eff}\frac{\partial U}{\partial x}\right)+\frac{1}{r^n}\frac{\partial}{\partial y}\left(r^n\,\mu_{eff}\frac{\partial V}{\partial x}\right)$
y-momentum	V	μ_{eff}	$-\frac{\partial p}{\partial y}+\frac{\partial}{\partial x}\left(\mu_{eff}\frac{\partial U}{\partial y}\right)+\frac{1}{r^n}\frac{\partial}{\partial y}\left(r^n\,\mu_{eff}\frac{\partial V}{\partial y}\right)-n\frac{2\mu_{eff}V}{r^2}$
Transport of k	k	$\mu+\dfrac{\mu_t}{\sigma_k}$	$\rho P-\rho\varepsilon$
Transport of ε	ε	$\mu+\dfrac{\mu_t}{\sigma_\varepsilon}$	$C_{\varepsilon1}\dfrac{\rho\varepsilon}{k}P-C_{\varepsilon2}\dfrac{\rho\varepsilon^2}{k}$

Table 3. Constants adopted by the standard k-ε model,
Launder and Spalding [12]

C_μ	$C_{\varepsilon1}$	$C_{\varepsilon2}$	σ_k	σ_ε
0.09	1.44	1.92	1.0	1.3

4.2. Boundary Conditions

The boundary conditions required to solve the system of governing differential equations are presented in this section. Generally there are four types of boundaries: inlet, outlet, symmetry axis and solid walls.

Inlet. A uniform velocity profile is prescribed at the inlet. Values of k and ε are estimated according to the equations: $k_{in}=1.5(IU_{in})^2$ where U_{in} is the average inlet velocity and I is the turbulence intensity $(=3\ \%)$ and $\varepsilon=C_\mu(k^{3/2})/0.05\,D$ for the conical diffuser and $\varepsilon_{in}=C_\mu k^{3/2}/(0.3\,W_1)$ for the two-dimensional diffuser.

Outlet. Downstream the diffuser, the flow extends over a sufficiently long domain so that it is fully developed at the exit section. Thus for any variable ϕ. the axial gradient is presumed to be zero, $\partial\phi/\partial x=0$.

Symmetry axis. On the symmetry axis, the radial derivative for any variable ϕ, vanishes, so that $\partial\phi/\partial y=0$.

Solid walls. At the wall boundaries, the no-slip conditions are applied.

4.3. Fluid Flow Solution Procedure

The CAFFA is a body-fitted finite-volume code with a collocated variable arrangement. The pressure and mean velocity fields are coupled with the iterative SIMPLE algorithm, Patankar [13]. to promote the solution of the pressure field. The treatment of the momentum equations at wall boundaries has been achieved by the wall function approach of Launder and Spalding [12]. An upwind-differencing scheme is used for the discretization of the governing equations. The linear equation systems arising from discretization are solved with the strongly implicit procedure of Stone [14]. Converged solutions are accepted when the absolute residual sums, normalized by the inlet fluxes, are below 10^{-4} for all variables.

5. OBJECTIVE FUNCTION

The working principle of diffusers is to obtain a static pressure rise through deceleration of the fluid by area enlarging. Depending on the particular diffuser installation, the primary objective can be either a velocity-decrease (the diffuser is placed after the test-section discharge of a closed-circuit wind tunnel to decrease power requirements), a pressure-increase (the use of a diffuser downstream of a turbine), or to supply a downstream process with a steady, uniform flow (the diffuser is placed immediately before a turbomachine). In the present work, the design objective is maximizing the static pressure rise.

The diffuser performance is characterized by the static pressure recovery. The static pressure recovery coefficient C_p can be defined as the ratio of the static pressure rise through the diffuser to the dynamic pressure at the diffuser inlet:

$$C_p = \frac{p_{Ex} - p_{In}}{0.5\,\rho\,U_{In}^2} \qquad\qquad \text{.... (4)}$$

where p_{In} and p_{Ex} are the average static pressures at the inlet and outlet of the diffuser, respectively. ρ is the fluid density and U_{In} is the average inlet velocity.

It is well known that for diffusers with tailpipe discharge, the static pressure continues to rise slightly beyond the diffuser exit as the velocity distribution changes. Experimental investigations have shown that the position of maximum pressure varies with divergence angle and other factors, and that it occurs between two and six outlet diameters downstream the exit in conical diffusers (Cockrell and Markland [15]). It is chosen to determine the inlet and outlet pressures at the entry plane of the diffuser and the plane of the maximum pressure in the tailpipe, respectively.

6. OPTIMIZATION ALGORITHM

The technique used in this study for the optimization of two-dimensional diffusers is based on Genetic Algorithms (GA) (Goldberg, [16]). GAs are search procedures based on the mechanics of natural genetics in that a population of artificial individuals exchanges information to eventually adapt itself to set conditions according to the "survival of the fittest" principle.

6.1. Overview of Genetic Algorithms

Genetic algorithms are stochastic numerical search procedures inspired by biological evolution, cross-breeding trial solutions and allowing only the fittest solutions to survive and propagate to successive generations. They deal with a population of individual (candidate) solutions, which undergo constant changes by means of genetic operations of reproduction, crossover, and mutation. These solutions are ranked according to their fitness with respect to the objective function where the fit individuals are more likely to reproduce and propagate to the next generation. Based on their fitness values, individuals (parents) are selected for reproduction of the next generation by exchanging genetic information to form children (crossover). The parents are then removed and replaced in the population by the children to keep a stable population size. The result is a new generation with (normally) better fitness. Occasionally, mutation is introduced into the population to prevent the convergence to a local optimum and help generate unexpected directions in the solution space.

6.2. Components of Genetic Algorithms

Standard genetic algorithms involve three basic functions: selection, crossover, and mutation. Each function is briefly described below.

Selection – Individuals in a population are selected for reproduction according to their fitness values. In biology, fitness is the number of offspring that survive to reproduce. Given a population consisting of individuals identified by their chromosomes, selecting two chromosomes as parents to reproduce offspring is guided by a probability rule that the higher the fitness an individual has, the more likely the individual is selected. There are many selection methods available including weighted roulette wheel, sorting schemes, proportionate reproduction, and tournament selection.

Crossover – Selected parents reproduce the offspring by performing a crossover operation on the chromosomes (cut and splice pieces of one parent to those of the other). In nature, crossover implies two parents exchange parts of their corresponding chromosomes. In genetic algorithms, crossover operation makes two strings swap their partial strings. Since more fit individuals have a higher probability of producing offspring than less fit ones, the new population will possess on average an improved fitness. The basic crossover is a one-point crossover. Two selected strings create two offspring strings by swapping the partial strings, which are cut by one randomly sampled breakpoint along the chromosome. The one-point crossover can be easily extended to k-point crossover. It randomly samples k breakpoints on chromosomes and then exchanges every second corresponding segments of two parent strings.

Mutation – Mutation is an insurance policy against lost bits. It works on the level of string bits by randomly altering a bit value. With small probability, it randomly selects one bit on a chromosome then inverts the bit from 0 to 1 or vice versa. The operation is designed to prevent GA from premature termination, namely converging to a solution too early.

6.3. Micro-Genetic Algorithm

In the present study, the optimization algorithm is based upon a Genetic Algorithm. The program was developed by David Carroll [17], [18]. Reproduction and mutation take place using the micro-genetic algorithm (μ-GA) technique with elitist strategy (Krishnakumar, [19]). The population size is fixed at only 5 individuals: since a strong crossover enriches diversity in the new population of strings, crossover is used with a probability of one and the mutation rate is kept at zero. This means that all the new five individuals are obtained through uniform crossover and none of them comes from the mutation of an individual of the old population. However, mutation still acts on the bits of the offspring with a low probability (0.005). The GA configuration used is illustrated in Table 4.

Table 4. The GA configuration used

GA Technique	μ-GA with elitism
Population size	5 individuals
Offspring by crossover	100%
Offspring by mutation	0%
Mutation probability	0.005
Bits per parameter	10

7. APPLICATIONS

In the design of diffusers, different optimization problems could be identified, Kline et al. [20]. Among these, the following two cases are investigated:

1. Maximum pressure recovery for a given area ratio (AR) regardless of length in the flow direction. A conical diffuser is designed in this study according to the data given by Eisinger and Ruprecht [8].
2. Maximum pressure recovery through diffuser wall contouring with given AR and L/W_1. This case study is for a two-dimensional diffuser and it was adopted from Madsen et al. [6].

In the two cases, the flow is assumed to be steady turbulent incompressible flow. Due to symmetry, only the symmetric half of the diffuser is considered in the numerical analysis. The diffuser centerline has symmetry boundary conditions and the upper wall is a no-slip wall.

The formulation of the optimization problem is as follows. The objective of the design optimization is to find the values of the design variables with the consideration of various constraints in such a way that an objective function attains a maximum value. The design constraints are determined by feasibility considerations for each parameter. The constraints are driven by functional restrictions and the Reynolds number is kept constant.

7.1. Length of Axially Symmetric Diffuser

The first problem examined is that of determining the length of an axisymmetric diffuser that leads to the maximum pressure rise under certain flow, boundary and geometry constraints. The geometry constraints, Fig. 2, are: prescribed inlet diameter D (= 0.15 m), constant length of inlet and outlet sections of values $L_{in} = D$ and $L_{ex} = D$, respectively. The diffuser area ratio is 4. A uniform velocity profile is specified at the inlet, $U_{in} = 10$ m/s, and the inlet Reynolds number based on the inlet diameter is $Re = 10^5$. The aim is to estimate the conical diffuser length, L, that gives the maximum pressure recovery coefficient. The maximum length of the diffuser is limited to 12 D, which corresponds to a total divergence angle, 2α, of 4.8 deg. The behavior of the genetic algorithms is tested and the only parameter (degree of freedom), which will be optimized, is the length of the diffuser.

Therefore, the considered problem has:

Objective function	$F = C_p$
Parameters (design variables)	L
Design constraints	$0 < L \le 12 D$

Grid Independence Tests

A grid refinement study is performed to ascertain the grid resolution required for the optimization. For a selected diffuser with $L/D = 8$, three sets of grids are used: a coarse grid of 70 x 15 (1,224 grid points), a medium grid of 100 x 30 (3,264 grid points) and a fine grid of 140 x 40 (5,964 grid points). Each grid set is in the longitudinal and radial directions, respectively, and the grids are refined near the walls and at the regions with high gradients. Figure 3 illustrates the variation of the pressure recovery coefficient along the diffuser and the tailpipe, and the gain in the C_p through the tailpipe. The difference in C_p values between the medium and fine grids is small. Based on this grid selection study, an effectively grid independent solution is achieved by the fine grid. All results presented here are for the fine grid.

It is worthy to mention that as the optimization tool chooses the length of diffuser, the number of grids in the longitudinal direction of the diffuser is tuned to be sure that the resulted grid is properly achieved to obtain grid independent solution.
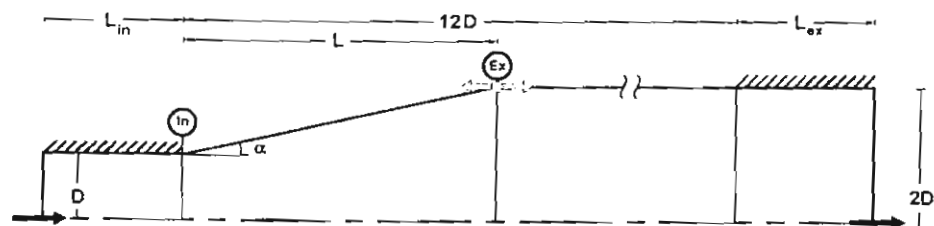

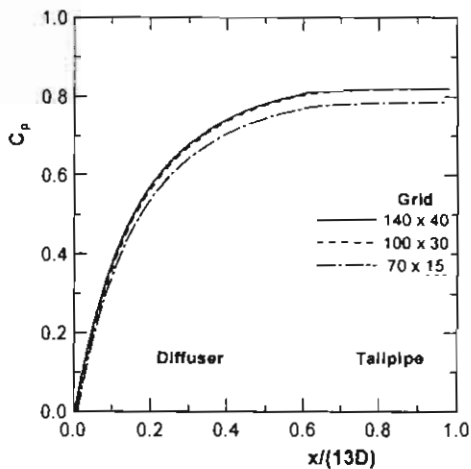Figure 2. Axisymmetric diffuser with one degree of freedom (shown arrows at Ex)

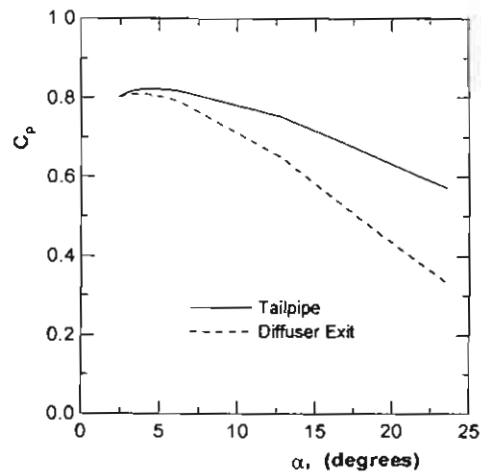Figure 3. Effect of grid density on pressure recovery coefficient

Figure 4. Pressure recovery coefficient rise in the tailpipe

Effect of the Tailpipe

Experimental results of the effect of the length of the tailpipe on C_p have been reported by Miller [21]. It is observed that the presence of a tailpipe is most beneficial in diffusers of larger area ratios and wider divergence angles. Conversely, for small divergence angles and small area ratios the presence or absence of a tailpipe has only a small effect on C_p. The outlet pipe or passage length to obtain maximum static pressure recovery is typically of the order of four diameters. For diffusers with tailpipe, it has been found that C_p is relatively insensitive to the entry velocity profile.

For the studied case, Figure 4 illustrates the variation with the diffuser half divergence angle of the pressure recovery coefficients at the diffuser exit and at the section of the maximum mean static pressure in the tailpipe. As observed earlier from Fig. 3, the static pressure continues increasing in the tailpipe. The increment in C_p in the tailpipe is noticeable and great with large diffuser angles. The values of C_p coefficients at the tailpipe are used in the optimization.

Optimization Results

For diffusers of a given area ratio, there is a value of the length parameter L/D for which C_p is a maximum. This maximum is denoted by C_p^{**} and its loci has been drawn on diffuser performance charts, Ward-Smith [22]. In Figure 5, the calculated pressure recovery coefficients for arbitrarily selected diffuser lengths by the optimization runs are plotted. After 35 calculations of different diffuser lengths the micro-genetic algorithm obtained the optimum length.

From Figure 5, it can be noticed that at a length of about 6.5 times the inlet diameter, the change in C_p is very small. The maximum pressure recovery coefficient obtained by optimization is 0.8223 at $L/D = 6.433$. This value corresponds to a total divergence angle, 2α, of 8.88 deg. To make a comparison with the available experimental results for conical diffusers with tailpipe discharge. the diffuser performance charts given by Ward-Smith [22] and Ishikawa and Nakamura [23] are

used.   According to the performance chart of Ward-Smith and for an area ratio of 4, the C_p^{**} line gives $L/D = 7.8$ and 2α of 7.34 deg, while Ishikawa and Nakamura performance chart gives $L/D = 14.32$ and the angle 2α is 4 deg. Both experimental data give C_p^{**} of 0.85. The big difference in the results of the previous experimental works is attributed to the blockage of the inlet velocity profile, the Reynolds number, and the tailpipe length.

Figure 6 illustrates the variation of the pressure recovery coefficient C_p obtained by the optimization runs with half the divergence angle of the diffuser. Also, the pressure recovery coefficients obtained from the equations proposed by Ishikawa and Nakamura [23] are shown.   They give the C_p coefficients at the section of the maximum pressure in the tailpipe for conical diffusers with $2° < \alpha < 15°$ and having a fixed stall and no appreciable stall, respectively, as:

$$C_p = 0.891 - 0.00097\alpha - 0.00073\alpha^2 \quad\quad\quad .... (5)$$

$$C_p = (0.912 - 0.0008\alpha - 0.00047\alpha^2)(1 - AR^{-2}) \quad\quad\quad .... (6)$$

The region between these two equations is for diffusers with transitory stall, Fig. 6.

The numerical simulations of the flow field show that for small half divergence angles $(\alpha < 6.5°)$ there is no appreciable stall, while with values greater than that value there is transitory stall. C_p values obtained by Eq. (6) for the no appreciable stall is higher than the numerical value of this study, Fig. 6. This can be attributed to the long tailpipe ($> 20\,D$) used in Ishikawa and Nakamura experiments compared to the tailpipe length used in this study ($L_\alpha + 12\,D - L$) which depends on the selected diffuser length during the optimization. In the transitory stall region, it is believed that there is an overestimation of the numerical values of C_p. This is on account of the previous observations, [24]-[27], that the k-ϵ turbulence model, among other models, overestimates C_p due to the underestimation of the reattachment length of the separation region.
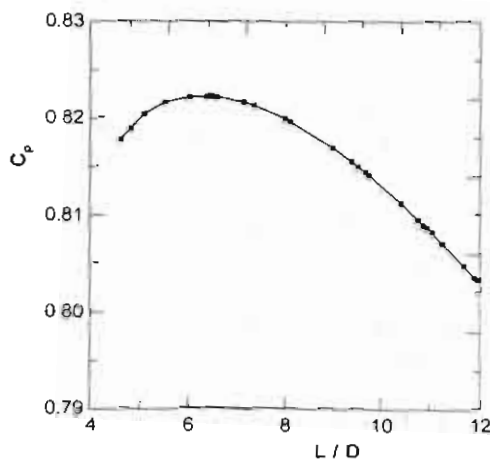

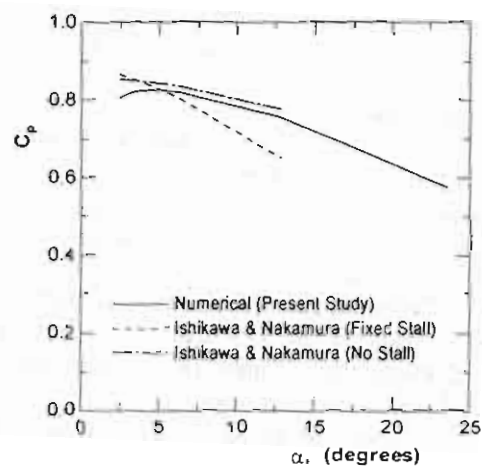Figure 5. Pressure recovery coefficient variation with the length ratio

Figure 6. Pressure recovery coefficient variation with half the divergence angle

7.2. Two-Dimensional Diffuser Wall Contouring

The second case is the achievement of maximum pressure recovery through wall contouring of a two-dimensional diffuser with given area ratio and length to height ratio. The baseline diffuser corresponds to the proposed configuration of Madsen et al. [6]. The geometry of the two-dimensional diffuser and its details are shown in Fig. 7. The geometry consists of an inlet section, a diffuser and an outlet section. The inlet width W_1 is taken as 0.15 m and the exit width W_2 as 0.3 m. Therefore, the diffuser has an area ratio $AR = 2.0$. The diffuser length $L = 1.5 W_1$ and the total divergence angle, 2α, is 36.9 deg. Inlet and outlet sections of lengths $L_{in} = 0.5 W_1$ and $L_{ex} = 3.5 W_1$, respectively, are attached to the diffuser to get uni-directional flow at the inlet and the exit.

The inlet flow conditions to the diffuser are prescribed in the straight duct at L_{in} upstream of the diffuser inlet. The uniform inlet velocity U_{in} is 10 m/s. The Reynolds number based on the inlet width of the diffuser is 10^5.

Diffuser wall parameterizations can be achieved by using polynomial functions or parametric curves such as B-splines and Bezier curves. Polynomial functions are chosen to represent the two-dimensional diffuser contour because they are simple curve representation. Polynomials are often considered impractical for design optimization because of a tendency to produce undesirable wiggles. For diffusers, this problem is eliminated by enforcing analytically derived conditions of curve monotonicity, (Madsen et al. [6]).

The diffuser wall contour is defined by a fourth-order polynomial:

$$y(x) = a_4 x^4 + a_3 x^3 + a_2 x^2 + a_1 x + a_0 \qquad \qquad \dots (7)$$

The polynomial curve must pass through four points: the inlet point (In), the two control points (1) and (2) and the exit point (Ex), Fig. 7. The two control points define the shape as well as the curvature of the inlet and outlet edges of the diffuser. Each coordinate for the control point could take a value inside a predetermined range defining a family of "realistic" shapes. In the present study, the abscissas of the control points are uniformly spaced along the diffuser length, i.e., $x_1 = 0.5 W_1$ and $x_2 = W_1$. The ordinates of the two control points y_1 and y_2 are the design variables and they are chosen inside a fixed range of acceptable values. At the diffuser inlet, the wall contour is C^1-continuous to avoid a sharp edge entrance, which may lead to undesirable onset of separation. This tangent continuity gives the condition of zero slope $dy/dx = 0$ at
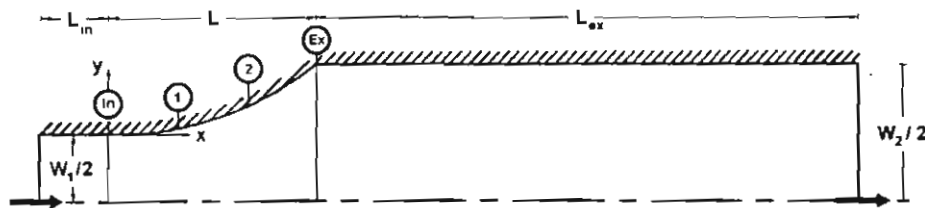

Figure 7. Baseline 2-D diffuser

the diffuser inlet ($x = 0$). Applying this condition, the polynomial function is reduced to:

$$y(x) = a_4 x^4 + a_3 x^3 + a_2 x^2 \qquad\qquad \text{.... (8)}$$

The coordinates of the two control points and the exit point are used to solve Eq. (8) and obtain the polynomial coefficients in terms of control point positions y_1 and y_2:

$$a_2 = \left(12 y_1 - 3 y_2\right)/W_1^2 + 2/\left(9 W_1\right)$$
$$a_3 = \left(-20 y_1 + 8 y_2\right)/W_1^3 - 2/\left(3 W_1^2\right)$$
$$a_4 = \left(8 y_1 - 4 y_2\right)/W_1^4 + 4/\left(9 W_1^3\right) \qquad\qquad \text{.... (9)}$$

Monotonicity Constraints

Experimental and numerical evidence indicates that maximum pressure recovery in diffusers occurs at the border of appreciable flow separation. For this reason, strongly separated diffuser flows should be avoided, making it reasonable to restrict the design space to monotonic wall shapes.

Based on experiments, Carlson et al. [28] established the highest pressure recovery coefficients from bell-shaped diffuser designs. This has been established by numerical optimization of diffusers with laminar flow, Çabuk and Modi [2] and Svenningsen et al. [3], and with turbulent flow, Madsen [29].

- The monotonicity in the position of control points yields:

$$0 \le y_1 \le y_2 \le W_1/2 \qquad\qquad \text{.... (10)}$$

- For a wall shape $y(x)$ to be monotonic, it is required that the first-order derivative does not change its sign:

$$\frac{dy}{dx} = x\left(4 a_4 x^2 + 3 a_3 x + 2 a_2\right) = x Z(x) > 0 \qquad \text{for} \quad 0 \le x \le 1.5 W_1$$

Since x is positive in the considered interval, it is sufficient for monotonicity that $Z(x)$ is positive in the same interval. The two conditions $Z(x = 0) > 0$ and $Z(x = 1.5 W_1) > 0$ yield:

$$y_2 < 4 y_1 + \frac{2}{27} W_1 \qquad\qquad \text{.... (11)}$$

$$y_2 < y_1 + \frac{13}{54} W_1 \qquad\qquad \text{.... (12)}$$

Figure 8 shows the ordinates of the two control points y_1 and y_2 non-dimensionalized by half the inlet height $W_1/2$. Both initial and reduced design spaces are depicted in Fig. 8. Equations (10)-(12) are represented by lines a, b and c, respectively. The initial design space is the upper triangle, while the reduced design is that given by the dotted surface.

Similar to the previous case, the considered problem has:

Objective function	$F = C_p$
Parameters (design variables)	y_1, y_2
Design constraints	Eqs. (10), (11) and (12)

Grid Independence Tests

Before starting the optimization, a grid refinement study was performed also on this case. For a 2-D diffuser with straight walls, the grids used were: 100 x 30 (3,264 grid points), 120 x 40 (5,124 grid points) and 130 x 50 (6,864 grid points). The fine grid achieves a grid independent solution; consequently it is used for the optimization runs.

Optimization Results

Figure 9 shows the hill chart of the pressure recovery coefficient for the non-dimensional parameters $2y_1/W_1$ and $2y_2/W_1$. It can be noticed that different diffuser shapes are found to yield essentially the same performance. The central region indicates the optimal region. The space with $C_p = 0.69$ comprises designs with performance within 0.08% of the optimal. For the maximum pressure recovery coefficient, there are multiple design points that meet this objective. Table 5 gives the non-dimensional parameters $2y_1/W_1$ and $2y_2/W_1$, the corresponding diffuser shapes without the inlet and outlet sections, and the streamlines.

The improvement in C_p over that for a straight walled diffuser represents the gain in pressure rise due to shaping of the diffuser with a polynomial curve. The straight wall diffuser with the same area ratio AR and Reynolds number is tested numerically and the obtained C_p is 0.6887. Comparing to the optimum profile diffuser's pressure recovery coefficient $C_p = 0.6908$, results in an improvement in C_p less than 1% which can be considered as very small gain. This is in consistent with the remarks of Madsen et al. [5] that the pressure recovery improves marginally for small area ratios and substantially for great values.
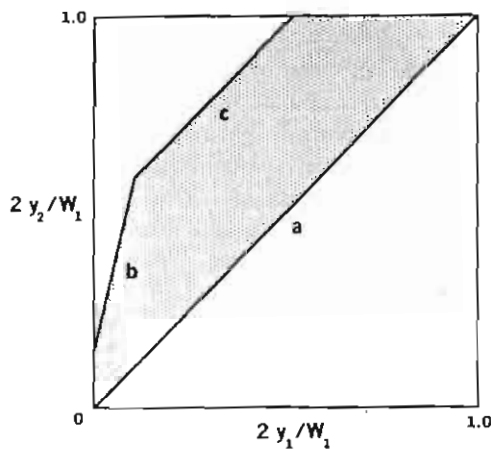

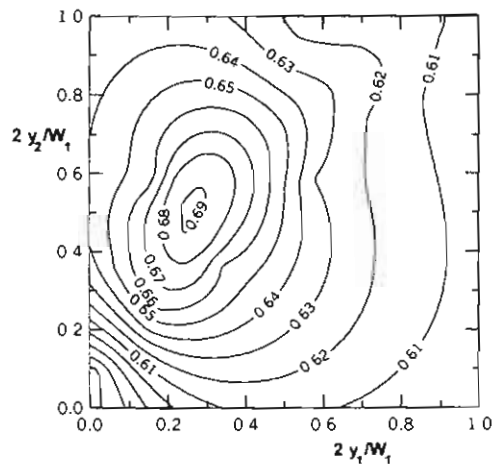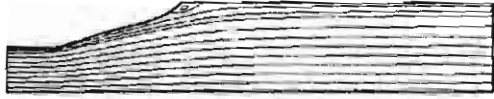Figure 8. Initial and reduced design spaces for Case 2
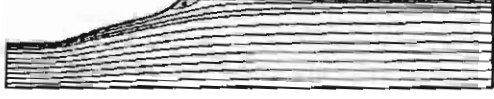

Figure 9. Hill chart of the pressure recovery coefficient for Case 2

Table 5. Optimum profile diffusers C_p, parameters, shape and streamlines

C_p	$2y_1/W_1$	$2y_2/W_1$	Diffuser Shape
0.6908	0.25013	0.51453	
0.6908	0.25733	0.51907	

The obtained numerical results are compared with those of Madsen et al. [5]: for the same area ratio but with a different Reynolds number. The study of Madsen et al. [6] gives the predicted optimum value of C_p equals to 0.7185 for $2y_1/W_1 = 0.3767$ and $2y_2/W_1 = 0.5333$. Applying these values of parameters for the code used in this study, the predicted C_p is 0.6788. The comparison of the values of C_p indicates that the code used by Madsen et al. [6] has a weaker tendency for flow separation. The difference between the two codes applying the same standard k-ε model could be explained by factors such as numerical diffusion and discretization schemes used in the two codes.

8. CONCLUSIONS

An automated design of two-dimensional and axisymmetric subsonic diffusers has been achieved. Three codes of fluid flow simulation (Grid, CAFFA and Plot) and an optimization tool using the micro-genetic algorithms have been coupled. The CFD model is based on the Reynolds-averaged Navier-Stokes equations, with the standard k-ε closure turbulence model. The objective of the optimization was to maximize the static pressure recovery coefficient. The optimization tool and the flow field simulation are evaluated through two test cases. The flow is incompressible and fully turbulent with a Reynolds number of 10^5, based on the inlet width. The obtained computational results are compared with existing experimental and computational data. The first case dealt with one degree of freedom: the length of a conical diffuser, and the second case is a two-dimensional contoured diffuser that was designed with two degrees of freedom: the vertical positions of the two control points of the wall surface.

The following conclusions may be drawn from the present study:

1- The design optimization tool is fully automated and it works smoothly providing improved subsonic diffuser geometries.

2- For the turbulent flow computation of the conical diffuser (case 1), the numerically predicted optimum diffuser pressure recovery coefficient is compared with experimental results. Good agreement is obtained in the region of no-appreciable

stall. The optimum conical diffuser divergence angle is 8.81 deg for an area ratio of 4.

3- Comparison of the straight-walled diffuser with the optimum profile diffuser (case 2), for an area ratio of 2, indicates that a minor improvement is achieved by wall contouring.

ACKNOWLEDGMENTS

NOMENCLATURE

AR	area ratio, W_2/W_1 for 2-D diffuser; D_2^2/D_1^2 for conical diffuser
$C_{\varepsilon 1}$, $C_{\varepsilon 2}$	constants in the k-ε model
C_μ	eddy viscosity coefficient
C_p	static pressure recovery coefficient
D_1	diameter of diffuser at inlet, (m)
D_2	diameter of diffuser at exit, (m)
F	objective function
I	turbulence intensity, (%)
k	turbulent kinetic energy, (m²/s²)
L	length of diffuser, (m)
n	superscript in Eq. (1): for axisymmetric: $n = 1$; for 2-D: $n = 0$
P	turbulence energy generation rate, (m²/s³)
p_{Ex}	average static pressure at the diffuser exit, (Pa)
p_{In}	average static pressure at the diffuser inlet, (Pa)
Re	Reynolds number, $\rho U_{In} W_1 / \mu$
U	mean streamwise velocity component, (m/s)
U_{In}	average inlet velocity, (m/s)
V	mean transverse velocity component, (m/s)
W_1	width of diffuser at inlet, (m)
W_2	width of diffuser at exit, (m)
x_1	abscissa of the first control point, (m)
x_2	abscissa of the second control point, (m)
y_1	ordinate of the first control point, (m)
y_2	ordinate of the second control point, (m)
α	divergence angle, $[AR = 1 + 2(L/W_1)\tan\alpha$ for 2-D diffuser; $\sqrt{AR} = 1 + 2(L/D_1)\tan\alpha$ for conical diffuser], (deg)
ε	dissipation rate, (m²/s³)
μ	laminar viscosity of fluid, (Pa.s)
μ_{eff}	effective viscosity, (Pa.s)

μ_t turbulent viscosity, (Pa.s)

ρ density of fluid, (kg/m^3)

σ_k, σ_ε turbulent Prandtl numbers in k and ε transport equations

REFERENCES

1- Lefantzi, S., and Knight, D.D., "Automated Design Optimization of a Three-Dimensional S-Shaped Subsonic Diffuser," *Journal of Propulsion and Power*, Vol. 18, No. 4, pp. 913-921, 2002.

2- Çabuk, H., and Modi, V., "Optimum Plane Diffusers in Laminar Flow," *Journal of Fluid Mechanics*, Vol. 237, pp. 373-393, 1992.

3- Svenningsen, K.H., Madsen, J.I., Hassing, N.H., and Päuker, W.H.G., "Optimization of Flow Geometries Applying Quasi-Analytical Sensitivity Analysis," *Applied Mathematical Modelling*, Vol. 20, No. 3, pp. 214-224, 1996.

4- Cholaseuk, D., Srinivasan, V., and Modi, V., "Shape Optimization for Fluid Flow Problems Using Bezier Curves and Designed Numerical Experiments," *Proceedings of the 1999 ASME Design Engineering Technical Conferences*, Las Vegas, Nevada, September 12-15, 1999. Paper No. DETC99/CIE-9116. (http://www2.engr.tu.ac.th/~cdulyach/DETC99/CIE-9116.pdf).

5- Madsen, J.I., Olhoff, N., and Condra, T.J., "Optimization of Straight, Two-Dimensional Diffusers by Wall Contouring and Guide Vane Insertion." *Proceedings of the 3rd ISSMO/UBCAD/UB/AIAA World Congress of Structural and Multidisciplinary Optimization*, WCSMO-3, Buffalo, NY, USA, May 17-21, 1999. (http://www.eng.buffalo.edu/Research/MODEL/wcsmo3/proceedings/43EOA3/43EOA33.pdf).

6- Madsen, J.I., Shyy, W., and Haftka, R.T., "Response Surface Techniques for Diffuser Shape Optimization," *AIAA J.*, Vol. 38, No. 9, pp. 1512-1518, 2000.

7- Cholaseuk, D., Srinivasan, V., and Modi, V., "Robustness in Optimum Design of Freeform Mechanical Parts," *Proceedings of DETC'00. ASME 2000 Design Engineering Technical Conferences and Computers and Information in Engineering Conference*, Baltimore, Maryland, September 10-13, 2000. Paper No. DETC2000/CIE-14652. (http://www2.engr.tu.ac.th/~cdulyach/DETC2000-CIE-14652.pdf).

8- Eisinger, R., and Ruprecht, A., "Automatic Shape Optimization of Hydro Turbine Components Based on CFD," *Seminar "CFD for Turbomachinery Applications"*, Gdansk, September 2001. (http://www.ihs.uni-stuttgart.de/forschung/veroeff/stroem/v2001_05.pdf).

9- Lund, E., Møller, H., and Jakobsen, L.A., "Shape Design Optimization of Stationary Fluid-Structure Interaction Problems with Large Displacements and Turbulence," *Proc. 4th World Congress on Structural and Multidisciplinary Optimization*, (Editor G. Cheng), 4-8 June, 2001, Dalian, China. (http://www.ime.auc.dk/people/employees/el/ps/153I.pdf)

10- Madsen, J.I., and Langthjem, M., "Multifidelity Response Surface Approximations for the Optimum Design of Diffuser Flows." *Optimization and Engineering*, Vol. 2, pp. 453-468, 2001.

11- Ferziger, J.H., and Perić, M., *Computational Methods For Fluid Dynamics*,

Springer-Verlag. 1996.

12- Launder, B.E.. and Spalding. D.B.. "The Numerical Computation of Turbulent Flows," *Computer Methods in Applied Mechanics and Engineering*, Vol. 3, Part 3, pp. 269-289, 1974.

13- Patankar, S.V.. *Numerical Heat Transfer and Fluid Flow*, McGraw-Hill. New York, 1980.

14- Stone, H.L., "Iterative Solution of Implicit Approximation of Multi-Dimensional Partial Differential Equations," *SIAM Journal of Numerical Analysis*, Vol. 5, No. 3, pp. 530-558, 1968.

15- Cockrell, D.J., and Markland, E., "A Review of Incompressible Diffuser Flow," *Aircraft Engineering*, Vol. 35, pp. 286-292, 1963.

16- Goldberg, D.E., *Genetic Algorithms in Search, Optimization and Machine Learning*, Addison Wesley, Reading, MA, 1989.

17- Carroll D.L., "Genetic Algorithms and Optimizing Chemical Oxygen-Iodine Lasers," *Developments in Theoretical and Applied Mechanics*, Vol. XVIII, (Eds. H. Wilson, R. Batra, C. Bert, A. Davis, R. Schapery, D. Stewart, and F. Swinson), School of Engineering. The University of Alabama, Alabama, pp. 411-424, 1996.

18- Carroll, D., "FORTRAN Genetic Algorithm Driver Program", 2001. (http://cuaerospace.com/caroll/ga.html).

19- Krishnakumar, K., "Micro-Genetic Algorithms for Stationary and Non-Stationary Function Optimization," *Proc. Soc. Photo-Opt. Instrum. Eng. (SPIE) on Intelligent Control and Adaptive Systems*, Vol. 1196, Philadelphia, PA, pp. 289-296, 1989.

20- Kline, S.J., Abbott, D.E., and Fox, R.W., "Optimum Design of Straight-Walled Diffusers," *ASME Journal of Basic Engineering*, Vol. 81, pp. 321-329, 1959.

21- Miller, D. S., *Internal Flow Systems. Design and Performance Prediction*, 2nd Edition, Gulf Publishing Company, Houston, 1990.

22- Ward-Smith, A.J., *Internal Fluid Flow. The Fluid Dynamics of Flow in Pipes and Ducts*, Clarendon Press, Oxford, pp. 336-341, 1980.

23- Ishikawa, K., and Nakamura, I., "Performance Chart and Optimum Geometries of Conical Diffusers with Uniform Inlet Flow and Tailpipe Discharge." *JSME International J.*, Series II, Vol. 33, No. 1, pp. 97-105, 1990.

24- Hah, C., "Calculation of Various Diffuser Flows with Inlet Swirl and Inlet Distortion Effects," *AIAA J.*, Vol. 21, No. 8, pp. 1127-1133, 1983.

25- Nitsche, W., and Haberland, C., "On Turbulent Separated Flows in Axisymmetric Diffusers," *Notes on Numerical Fluid Mechanics*. Vol. 40, (Vieweg, Braunschweig), "Physics of Separated Flows – Numerical, Experimental, and Theoretical Aspects", pp. 116-124, 1993.

26- Johnston, J.P.. "Review: Diffuser Design and Performance Analysis by Unified Integral Method (Data Bank Contribution)." *ASME Journal of Fluids Engineering*. Vol. 120, pp. 6-18, March 1998.

27- Test Case 8.2. "Flow Through an Asymmetric Plane Diffuser". *Proceedings of the 8th ERCOFTAC/IAHR/COST Workshop on Refined Turbulence Modelling*. Report 127, (Eds. A. Hellsten and P. Rautaheimo), Helsinki University of Technology. Espoo, Finland, 17-18 June 1999.

(http://www.CFDThermo.hut.fi/workshop99.html).

28- Carlson, J.J., Johnston, J.P., and Sagi, C.J., "Effects of Wall Shape on Fluid Regimes and Performance in Straight, Two-Dimensional Diffusers," *ASME Journal of Basic Engineering*, Vol. 89, pp. 151-160, March 1967.

29- Madsen, J.I., "Design Optimization of Internal Flow Devices," Ph.D. Dissertation, Institute of Energy Technology and Institute of Mechanical Engineering, Aalborg University, Aalborg, Denmark, October 1998. (http://www.aub.auc.dk/phd/department15/text/madsen-jens-i.pdf).